# Polymer Chemistry

Accepted Manuscript


This is an *Accepted Manuscript*, which has been through the Royal Society of Chemistry peer review process and has been accepted for publication.

*Accepted Manuscripts* are published online shortly after acceptance, before technical editing, formatting and proof reading. Using this free service, authors can make their results available to the community, in citable form, before we publish the edited article. We will replace this *Accepted Manuscript* with the edited and formatted *Advance Article* as soon as it is available.

You can find more information about *Accepted Manuscripts* in the Information for Authors.

Please note that technical editing may introduce minor changes to the text and/or graphics, which may alter content. The journal's standard Terms & Conditions and the Ethical guidelines still apply. In no event shall the Royal Society of Chemistry be held responsible for any errors or omissions in this *Accepted Manuscript* or any consequences arising from the use of any information it contains.

ROYAL SOCIETY OF CHEMISTRY

www.rsc.org/polymers

Journal Name

ARTICLE

# Liquid crystalline side-chain triblock copolymers consisting of a nematic central subblock edged by photochromic azobenzene-containing fragments: synthesis, structure and photooptical behaviour†

Received 00th January 20xx,
Accepted 00th January 20xx

DOI: 10.1039/x0xx00000x

www.rsc.org/

N.I. Boiko*[a], M.A. Bugakov[a], E.V. Chernikova[a], A. A. Piryazev[b], Ya.I. Odarchenko[b,d], D.A. Ivanov[b,c], V.P. Shibaev[a]

For the first time symmetrical photosensitive fully liquid crystalline side chain triblock copolymers (pAzo-*b*-pPhM-*b*-pAzo) and random copolymer (pAzo-*ran*-pPhM) with nematogenic phenyl benzoate (PhM) and photosensitive smectogenic azobenzene containing groups (Azo) were synthesized by combination of RAFT polymerization and subsequent chemical modification. The central block of synthesized photochromic block copolymers contains 80 PhM groups, while the length of "peripheral" blocks includes 4 or 10 Azo units. The microphase separation structure is observed in block copolymer when the length of subblock with Azo groups reaches ten monomeric units. The influence of photochromic polymers molecular architecture (homopolymer, block copolymer and random copolymer) on the photochemical and photoorientation processes induced by light in their amorphous films have been revealed. The optical anisotropy induced in block copolymer films by illumination with linearly polarized 546 nm light was studied and the results compared with those of the Azo homopolymer and of a random copolymer with a similar composition. It was found that practically only Azo groups are included in the process of photoinduced orientation in films of block copolymer, whereas the orientational cooperative effect of both azobenzene chromophore and phenyl benzoate mesogenic groups is observed in the case of random copolymer.

## Introduction

In the last decades the interest to design and research into the "smart" materials regulated at molecular and supramolecular levels under external fields (e.g., electromagnetic, mechanical, thermal fields etc.) has been considerably growing. Liquid crystalline (LC) azobenzene-containing polymers belong to such materials capable of providing a fast response to the light action through a reversible photoinduced E-Z isomerization of azobenzene (Azo) chromophore accompanied by large changes occuring of its molecular size, shape, and polarity[1-3]. These structural changes may essentially influence on wettability,[4,5] phase transitions,[6-9] thin films contracting,[10-17] and surface modification[18-20] of polymers. Under irradiation by linearly polarized light the Azo chromophores are known to orient preferentially in the direction perpendicular to the polarization plane of the excitation light (Weigert effect[21]). This behavior is due to the repeated cycles E-Z-E isomerization induced by action of light and accompanied by rotational diffusion of the chromophore. Photoorientation processes result in the appearance of photoinduced optical anisotropy (birefringence and dichroism) which makes this type of photoresponsive materials interesting for many applications in the field of photonics and holography.[22-32]

Incorporation of Azo-containing segments into block copolymers (BCPs) in which the Azo moiety plays a role of a mesogen and a photosensitive chromophore presents a considerable interest. The combination of microphase-separated morphologies (e.g., lamellae, spheres, cylinders) inherent to block copolymers with anisotropy and photosensitivity of azobenzene moiety opens the possibility to design new light driven materials with optically controlled physical properties at various scales. These polymer materials are promising for different technical application, namely photonic memories, optical switching, volume holographic recording, surface-relief grating (SRG) formation etc.

A large number of Azo-containing LC block copolymers of different molecular architecture, such as side-chain polymers,[33-39] main-chain polymers,[40,41] dendritic polymers[42-46] with covalently attached, ionic linkage or through hydrogen bonding

[a] Faculty of Chemistry, Moscow State University, Leninskie gory, Moscow, 119991, Russia. E-mail: boiko2@mail.ru.
[b] Faculty of Fundamental Physical and Chemical Engineering, Lomonosov Moscow State University (MSU), GSP-1, Leninskie gory - 1, 119991 Moscow, Russia
[c] Institut de Sciences des Matériaux de Mulhouse, CNRS UMR 7361, 15, rue Jean Starcky, F-68057 Mulhouse, France
[d] Present address : School of Biological Sciences, Royal Holloway, University of London, Egham, Surrey, TW20 0EX, United Kingdom
†Electronic Supplementary Information (ESI) available: $^{1}$H and $^{13}$C NMR spectra, GPC, POM, DSC, WAXS, UV-visible spectroscopy data. See DOI: 10.1039/x0xx00000x

mesogenic groups have been synthesized and described. The majority publications devoted to Azo-containing LC di- and triblock copolymers focus on the side-chain rod-coil block copolymers composed of both LC and amorphous blocks. Such block copolymers have been synthesized, as a rule, by atom transfer radical polymerization (ATRP) or reversible addition-fragmentation chain transfer polymerization (RAFT).

For example, it has been shown[47] that LC diblock copolymer consisting of polystyrene and Azo-containing subblocks is able to alter the orientation of the microphase separated (MPS) cylinder structure of coiled polystyrene microdomains periodically dispersed in the Azo LC matrix in response to linearly polarized light (LPL). Photocontrolled microphase separation in 2D has been demonstrated for a monolayer of triblock copolymer composed of poly(ethylene glycol) and azobenzene-containing polymethacrylate blocks.[34] Nagano et al. reported time-resolved in-situ measurements of the photoinduced alignment changes of both smectic LC Azo-containing layers and coiled poly(butyl methacrylate) cylindrical microdomains in block copolymer array by X-ray scattering.[48]

On the other hand, there are only a few papers dealing with Azo-containing side-chain diblock copolymers composed solely of LC blocks[49-51] (i.e., so-called fully liquid crystalline block copolymers) that form various types of mesophases in the individual state. Y. Zhao at al. presented the first observation of photoinduced microphase separation in a BCPs composed of two side-chain LC polymers[50] due to the shape incompatibility of cis isomers of Azo moieties with an ordered LC phase. Azo-containing diblock copolymers that are composed of two different side-chain LC polymers were synthesized by RAFT polymerization in ref.[51] It was shown that the photoorientational cooperative effects can be effective even in the microphase-separated samples due to the interaction of the two different mesogens via the interface. The obtained data demonstrate the ability of such block copolymers to rearrange their microphase-separated supramolecular structures under the action of electromagnetic fields.

Thus, to our knowledge, no systematic investigations into the photochromic fully LC block copolymers has been reported. Meanwhile, the synthesis of such block copolymers opens broad potentialities for the molecular design of new generation polymers that are composed of chemically distinct LC side-chain subblock with their own functionality and properties. The investigations of the novel and well-defined fully LC block copolymers are necessary to understand the structure/property relationships and are important from the viewpoint of fundamental understanding and practical applications of these unique materials in photonics and optoelectronics.

In the light of these considerations, here we report on the synthesis by RAFT polymerization and characterization of a novel family of symmetrical fully LC acrylic side-chain triblock copolymers (Fig.1). The central subblock of synthesized block copolymers contains 80 phenyl benzoate mesogenic groups, while the length of "peripheral" terminal subblocks includes 4 or 10 azobenzene units.

Parallel to synthesis of the block copolymers we also obtained a random copolymer consisting of the same monomer units. The latter was prepared in order to determine the effect of the molecular structure of photochromic copolymers on their

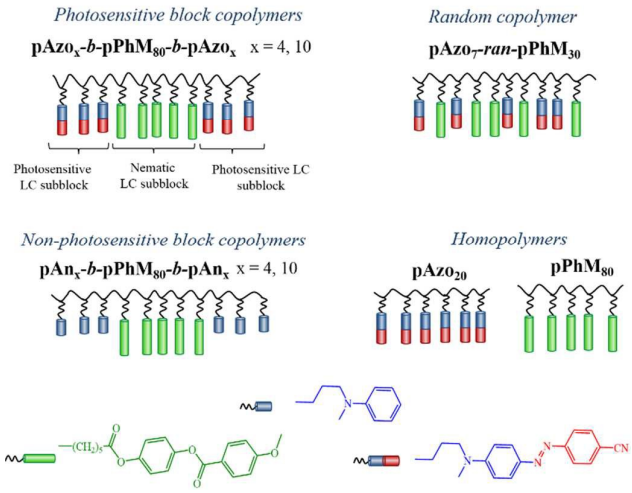


**Fig. 1** Chemical structures of the synthesized acrylic polymers.

physical-chemical properties. We also investigated "basic" homopolymers and block copolymers, containing methylaniline groups using in azocoupling reaction, as standards of comparison.

Of special interest is a comparative photooptical study of the triple block copolymers and statistical copolymers consisting of the same chemical components. It is well-known that the statistical azobenzene containing copolymers display cooperative orientational effect[24-25] under the light illumination that does not permit to control the optical properties of each individual components. However, the situation associated with triblock copolymers is not clear. We wanted to reveal a possibility of controlling the photooptical behaviour of only photochromic individual subblocks with their specific properties keeping the properties of the second component unchangable.

One of the reasons of Azo chromophores selection was the fact that the polymers containing these chromophores exhibit interesting properties, such as photo-induced anisotropy,[49, 52-54] SRG formation[18,19] and non-linear optical properties.[55-57]

## Experimental section

### Materials

Toluene, DMF, and ethyl acetate were dried over molecular sieves and distilled; THF and diethyl and petroleum ethers were distilled over KOH; anisole was boiled over sodium with benzophenone until the appearance of blue color and then distilled. Triethylamine and *N*-methylaniline were distilled under reduced pressure. An Ambersep 900 (the OH form) anion-exchange resin was purchased from Acros and was dried at 110°C in vacuum before use. AIBN was recrystallized from

anhydrous methanol before use. All other reagents were used as received except specially claimed.

#### Syntheses of the monomers and polymers

3-[methyl(phenyl)amino]propyl acrylate(compound A in Scheme 1) and transfer agent S,S'-bis(methyl-2-isobutyrate) trithiocarbonate (BMITC in Scheme 1) was synthesized as described in ref.[58, 59] 4-(6-Acryloyloxycapryloyloxyphenyl)-4-methoxybenzoate (monomer PhM in Scheme 1) was synthesized and purified according to the literature method.[60]
The synthetic details of triblock copolymers, $^1$H NMR spectra of the intermediate products, the monomers and polymers are given in the Electronic Supplementary Information (Fig. S1-S7†).The main characteristic of synthesized polymers are given in the Results and Discussion below.

#### Characterization

The molecular mass characteristics of the polymers were studied by SEC in THF using a chromatograph equipped with a Phenomenex 19 mm × 300 mm semi-preparative column packed with ultrastyragel with a pore size of 1000 Å and refractometric (Waters R-410) and UV-detectors. Molecular masses were calculated relative to PS standards. $^1$H NMR spectra of the polymers in the form of 3% solutions in $CDCl_3$ were measured on a Bruker DRX500 instrument.
The polarizing optical microscope (POM) investigations were performed using LOMO P-112 polarizing microscope equipped by Mettler TA-400 heating stage.
The phase transition temperatures of the polymers were studied by differential scanning calorimetry (DSC) with a PerkinElmer DSC-7 thermal analyzer with a scanning rate of 10 K/min. Samples were prepared as 10–20 mg pellets. Samples were first heated above isotropic melt to remove thermal history.
The microphase-separated structure was identified using atom force microscopy (AFM). The AFM experiments were performed on an FemtoScan instrument. The films were obtained by spin-coating method from the THF solution (25 mg/mL) of the triblock copolymer on glass substrates. After the solvent was removed at room temperature, the films were first annealed to 135 °C which was above the clearing point of the LC phase, and then slowly cooled to room temperature.
In-situ WAXS/SAXS experiments were performed using Xenocs WAXS/SAXS machine equipped with a GeniX3D generator (l =1.54Å) producing an X-ray beam of an approximately a 300x300μm$^2$ size. A Rayonix LX-170HS detector was used for WAXS data collecting, at a sample-to-detector distance of 20 cm. For SAXS data collecting Pilatus 300k detector was employed. The norm of the reciprocal space vector **s** ($|\mathbf{s}| = 2\sin\theta/\lambda$, where θ is Bragg angle and λ - wavelength) was calibrated using seven orders of Ag behenate for the WAXS region and three orders for the SAXS region. For data reduction and analysis, home-made programs designed in Igor Pro (Wavemetrics Ltd.) were used.
For photooptical experiments, thin polymer films were obtained by spin-coating from solutions of different concentration in THF. In order to completely remove any the traces of THF the spin-coated films were kept at room temperature for one day. The films were about 400 nm for homopolymers and 1.5 μm for copolymers. Measurements were carried out with profilometer.
Photochemical investigations were performed using an optical set up equipped with a DRSh-250 ultra-high pressure mercury lamp. Light with wavelength 404, 436 or 546 nm was selected using interference filter. To prevent heating of the samples due to IR irradiation of the lamp, water filter was used. The intensity of light was measured by LaserMate-Q (Coherent) intensity meter.
Spectral measurements were performed using Unicam UV-500 UV-Vis spectrophotometer. Ratio of E- and Z isomer in photostationary state of azobenzene-containing polymers in solutions and as-casted amorphous films was estimated by Fisher's method.[62] The linearly polarized spectra of the film samples were studied with a TIDAS spectrometer (J&M) equipped with rotating polarizer (Glan-Taylor prism controlled by computer program).
The dichroism values, D, of the polymer films were calculated from the spectra using the following equation:

$$D = \frac{A_\perp - A_\parallel}{A_\perp + A_\parallel} \qquad (1)$$

where $A_\parallel$ and $A_\perp$ are the optical absorptions at 422 nm or 260 nm measured with light linearly polarized in the direction parallel and perpendicular to the polarization of the exciting 546 nm light, respectively.

## Results and discussion

#### Homo- and block copolymer synthesis

For synthesis of triblock copolymers and random copolymers the combination of RAFT polymerization which was employed advantageously to synthesize symmetric acrylic triblock copolymers containing optically active cholesterol mesogenic groups[63] and a post-polymerization azo-coupling reaction described in[61] have been used (Scheme 1). Aiming at the controlled synthesis of LC symmetrical triblock copolymers we have applied RAFT polymerization using bifunctional symmetrical trithiocarbonate BMITC, the latter has been already successfully used for the RAFT polymerization of various vinyl monomers (e.g., acrylates, styrene, vinyl acetate, and acrylonitrile).[64]
The reversible chain transfer reactions occurring in the polymerization mediated by symmetric trithiocarbonates are as follows:

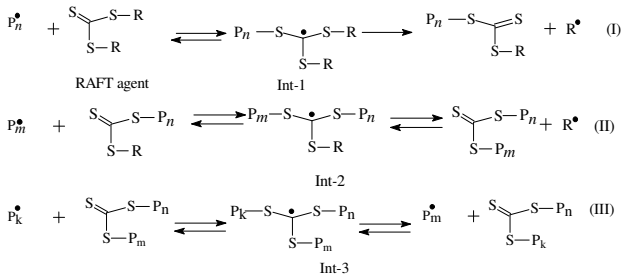


According to this mechanism, the "revival" of propagating radicals is provided by the multiple repetitions of reactions (II) and (III). Depending on the predominant way of chain "revival," the position of the trithiocarbonate group in a chain may differ.

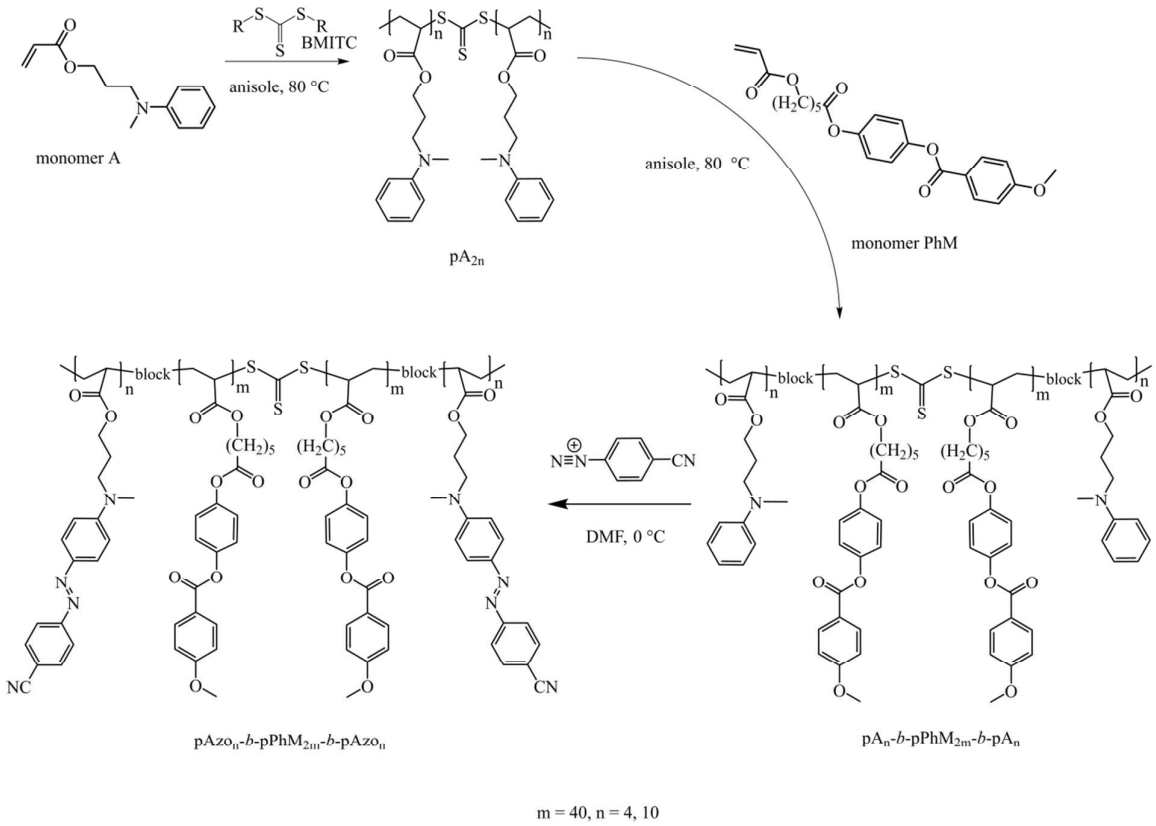


Scheme 1 General synthetic route for the azobenzene-containing fully LC symmetrical triblock copolymer.

If reaction (II) prevails, this group is located at the chain end; if reaction (III) predominates, this group sits within the chain. At a relatively low degree of polymerization, the position of the trithiocarbonate group may affect the properties of the polymer. However, it is well known that in conventional free-radical polymerization of acrylic monomers, the transfer reaction of propagating macroradicals to the azobenzene fragment occurs.[65] Our preliminary experiments revealed poor control over molecular mass characteristics of poly(3-[(4-[(4-cyanophenyl)diazenyl]phenyl)(methyl)-amino] propyl acrylate) in the presence of series of RAFT agents. This fact impelled us to use another strategy and the desired triblock copolymers were obtained (cf. Scheme 1) in three steps: 1) trithiocarbonate-mediated polymerization of monomer A, 2) block copolymerization of the monomer PhM in the presence of the resultant polymeric trithiocarbonate $pA_n$, and 3) the subsequent chemical modification of the resultant block copolymer via Azo-coupling reaction.

The first experiments discovered BMITC being more efficient RAFT agent among other representatives of trithiocarbonates.[58] The addition of 0.1 mol/L of BMITC to the polymerization of monomer A initiated by AIBN ($10^{-3}$ mol/L) led to the formation of oligomeric product, whose number average molecular mass

$M_n$ increased with the progress in monomer conversion (Table S1†) and was enough close to the theoretical value:

$$M_n = \frac{q[\mathrm{M}]_0}{[\mathrm{BMITC}]_0 + 2f[\mathrm{AIBN}]_0 e^{-k_i t}} \quad (2)$$

where $q$ is monomer conversion, $[M]_0$, $[BMITC]_0$, and $[AIBN]_0$ – molar concentrations of the monomer A, RAFT agent and initiator, respectively, $f$ – initiator efficiency, $k_i$ – initiation rate coefficient, and $t$ – polymerization time.[66]

The polymerization in this case proceeded relatively rapid: the limited conversions were reached during 2 h of heating at 80°C. However the PDI value slightly increased in the course of the polymerization, which in conditions of hundredfold molar excess of RAFT agent to initiator might be caused by the side reaction of the substituted amino group of monomer and the propagating radical.[67] The fact that PDI remains much lower than that of the polymers synthesized via conventional free radical

**Table 1** Molecular weights and distributions of the macromolecular chain transfer agents (homopolymers), triblock copolymers, and random copolymers obtained from GPC with calibrated polystyrene standards and $^1$H NMR

| | | DP ($A_n$) or ($Azo_n$)* | | Molar fraction of | DP ($PhM_n$) | |
|---|---|---|---|---|---|---|
| Polymers | $M_w/M_n$ | GPC | $^1$H NMR | block PhM** | GPC | $^1$H NMR |
| $pA_8$ | 1.17 | 8 | 6 | 0 | 0 | 0 |
| $pA_{20}$ | 1.36 | 20 | 19 | 0 | 0 | 0 |
| $pA_4$-*b*-$pPhM_{80}$-*b*-$pA_4$ | 1.55 | 8 | 6 | 0.9 | 80 | 70 |
| $pA_{10}$-*b*-$pPhM_{80}$-*b*-$pA_{10}$ | 1.52 | 20 | 19 | 0.8 | 80 | 80 |
| $pA_7$-*ran*-$pPhM_{30}$ | 1.35 | 7 | 9 | 0.8 | 30 | 40 |
| $pAzo_{20}$ | 1.39 | 20 | 19 | 0 | 0 | 0 |
| $pAzo_4$-*b*-$pPhM_{80}$-*b*-$pAzo_4$ | 1.55 | 8 | 6 | 0.9 | 80 | 70 |
| $pAzo_{10}$-*b*-$pPhM_{80}$-*b*-$pAzo_{10}$ | 1.52 | 20 | 19 | 0.8 | 80 | 80 |
| $pAzo_7$-*ran*-$pPhM_{30}$ | 1.41 | 7 | 9 | 0.8 | 30 | 40 |

*DP – degree polymerization. ** Determined by $^1$H NMR spectroscopy.

Journal Name

ARTICLE

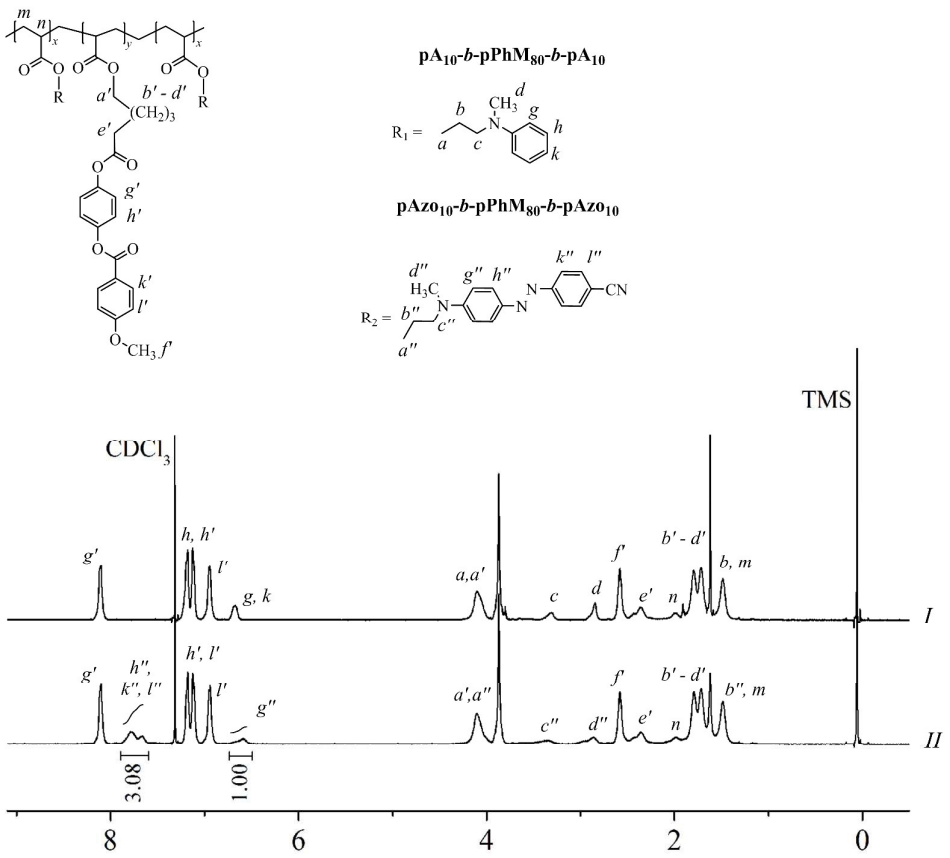


Fig. 2 $^{1}$H NMR spectra of block copolymers (*I*) $pA_{10}$-*b*-$pPhM_{80}$-*b*-$pA_{10}$ and (*II*) $pAzo_{10}$-*b*-$pPhM_{80}$-*b*-$pAzo_{10}$.

polymerization indicates that most of the polymeric chains are formed via reactions (I) – (III).

The chain extension confirms more reliably the living nature of the process. Hence two polymers $pA_n$ where n = 4, 10 (see Experimental section) containing active trithiocarbonate moiety have been used in solution polymerization of monomer PhM (1 mol/L) as polymeric RAFT agents. In this case the formation of symmetrical triblock copolymers $pA_n$-*b*-$pPhM_m$-*b*-$pA_n$ is expected, where the incorporation of monomer PhM units in the polymeric chain occurs between the sulfur atom of trithiocarbonate group and the terminal unit of polymeric substituent (see Scheme 1). It's necessary to note that as we have shown previously the trithiocarbonate group in initial homopolymer RAFT agents $pA_n$ is located virtually in the middle of the chain[58] and the structure of polymeric RAFT agents may be presented as $pA_n$–S–C(=S)–S–$pA_n$

As it is seen from the Table 1, the molecular mass distributions of the block copolymers are wider (polydispersity indexes of ~1.5) than those of initial polymers. Note that, in the RAFT polymerization of acrylic monomers in solution, a decrease in the monomer concentration usually leads to the same effect.[68] On the whole, it may be stated that $pA_n$ were efficient RAFT agents in the polymerization of monomer PhM and all block copolymers are enriched in monomer PhM units (Table 1). The chemical modification of the obtained block copolymers was conducted by the azocoupling reaction, in which a proton in the aromatic ring located in the *para*-position with respect to the nitrogen atom is replaced by an Azo group. The degree of conversion was quantified from the $^{1}$H NMR data (Figure 2). After chemical modification, the integral intensity of the peak at ~6.7 ppm corresponding initially to three protons of the aromatic ring decreased due to the reduction of the amount of

protons owing to replacement of protons situated in the *para*-position with respect to the amino group with an azo group during modification. Moreover, the chemical shift of protons located in the *meta*-position with respect to the amino group changes from ~7.1 ppm to ~7.7 ppm. This effect is associated with strong electron-acceptor properties of the incorporated fragment. Also ratio of integral intensities of the peaks at ~7.7 ppm and at 6.7 ppm is equal three that correspond to ratio of numbers of non-equal protons in azobenzene group. The above data indicated that the degree of substitution is close to 100%, and the desired triblock copolymers containing nematogenic phenyl benzoate and photosensitive azobenzene groups have been successfully synthesized. Note, there is no change in polydispersity index before and after the post polymerization modification. The molecular characteristics of all synthesized polymers estimated from data of GPC and $^1$H NMR spectroscopy are given in Table 1.

### Phase behavior

The phase behavior of the synthesized polymers was investigated by a combination of differential scanning calorimetry (DSC), thermal polarized microscopy (POM) and X-ray scattering. The phase transition temperatures of all samples were obtained from the first cooling (Fig. S8 and S9†) and second heating scans; the results are summarized in Table 2. DSC curves of the homopolymers are given in Fig. 3. Homopolymers $pA_{20}$ and $pA_8$ are amorphous and are characterized by a low glass transition temperature ($T_g$) close to - 28 °C and -25 °C respectively. After the post-polymerization Azo-coupling reaction the phase behavior of the homopolymers is sharply changed: $pAzo_{20}$ has a higher $T_g$ of 75°C and its DSC curve shows only one transition temperature at 155 °C (Fig. 3). In this temperature range the fan-shaped birefringent texture specific of smectic A (SmA) phase is observed (cf. microphoto in polarized light in Fig. S10a†). Homopolymer $pAzo_8$ has the same $T_g$ as $pAzo_{20}$.

Table 2. Thermal transition data and mesomorphic properties for the homopolymers, block and random copolymers prepared by RAFT and obtained from the second heating scans

| Polymers[a] | $T_g$, °C | Phase behaviour[b] (second heating), °C |
|---|---|---|
| $pPhM_{80}$ | 25 | N 125 ( 0.9) I |
| $pAzo_{20}$ | 75 | SmA 155 (2.2) I |
| $pA_4$-*b*-$pPhM_{80}$-*b*-$pA_4$ | 29 | N 119 (0.8) I |
| $pA_{10}$-*b*-$pPhM_{80}$-*b*-$pA_{10}$ | -1/28 | N 122 (0.9) I |
| $pAzo_4$-*b*-$pPhM_{80}$-*b*-$pAzo_4$ | 33 | N 122 (0.9)I |
| $pAzo_{10}$-*b*-$pPhM_{80}$-*b*-$pAzo_{10}$ | 33 | LC 136 (1.4) I |
| $pA_7$-*ran*-$pPhM_{30}$ | 21 | N 75 (0.7) I |
| $pAzo_7$-*ran*-$pPhM_{30}$ | 37 | N 108 (0.7) I |

[a]Subscripts indicate the polymerization degree of subblocks. [b]Mesophases: N is the nematic phase, SmA is the smectic phase A, and I is the isotropic melt. Isotropization enthalpy (in J/g) is given in brackets.

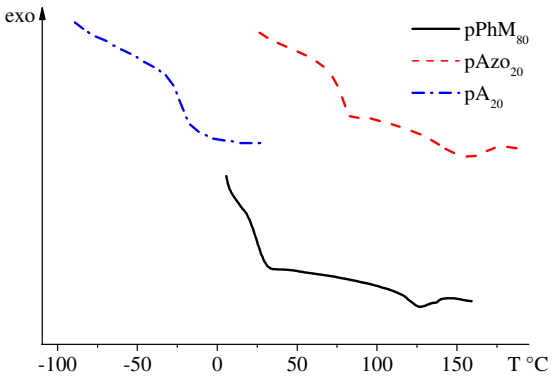


Fig. 3 DSC curves of the homopolymers $pA_{20}$, $pAzo_{20}$ and $pPhM_{80}$ obtained from the second heating scans.

To probe the structure of the Azo-containing homopolymers, X-ray scattering experiments were performed on uniaxially-aligned samples of $pAzo_{20}$ at room temperature. The samples were drawn from the polymer melt. Figures 4 a, b show diffraction patterns acquired on the fiber sample of $pAzo_{20}$. They display three sharp peaks positioned at 24.51, 12.27 and 8.17 Å and oriented along the equatorial direction on the pattern. Such peaks with a ratio of d-spacings of 1:2:3 indicate that the $pAzo_{20}$ homopolymer forms a SmA phase. In the wide-angle region, a diffuse diffraction peak corresponding to an average interatomic distance of 4.32 Å is visible. This peak likely corresponds to a disordered arrangement of the mesogenic groups within the smectic layers parallel to the fiber axis.

From the fit of the three orders of the fundamental smectic peak to a linear law, the smectic layer thickness at 25°C is estimated to be 24.51 Å. As the fully extended length of the Azo-containing monomer unit is calculated to be 21.19 Å, the side chains of the polymer are arranged according to the packing mode with fully interdigitated Azo-mesogens as depicted in Fig. 4c.

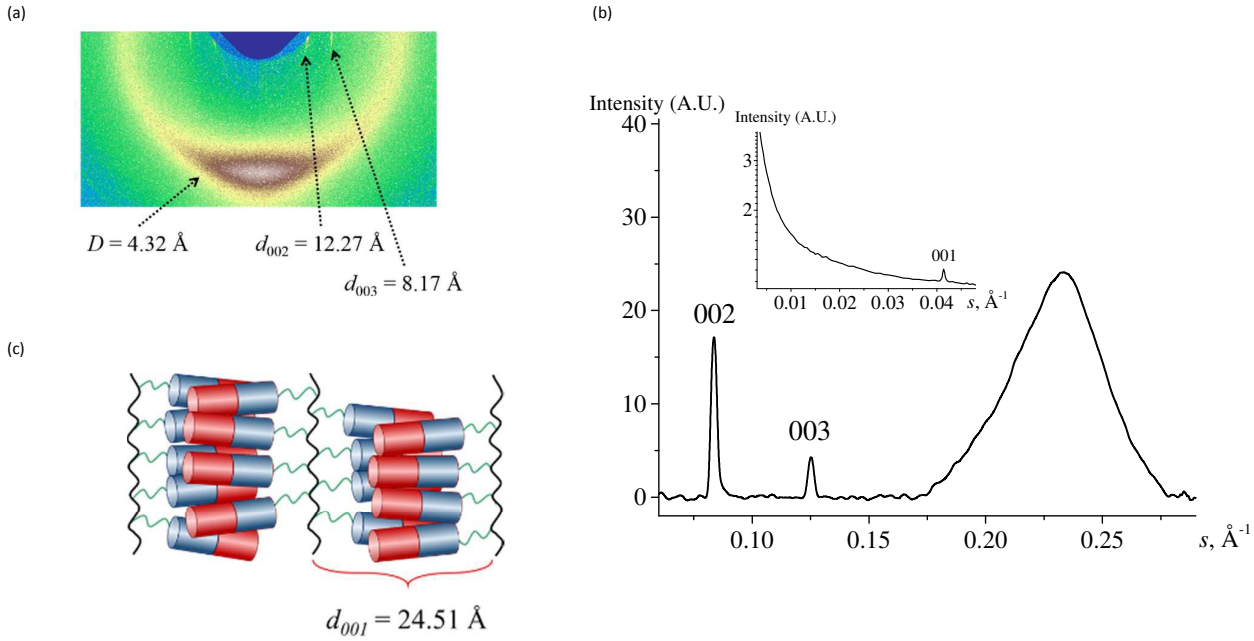


Fig. 4(a) 2D WAXS pattern corresponding to the fiber sample of $pAzo_{20}$, (b) 1D WAXS and SAXS (inset) diffractograms of $pAzo_{20}$, (c) scheme of the side-groups arrangement in the SmA phase of homopolymer $pAzo_{20}$ (fiber axis is vertical).

According to POM data (Fig. S10b†) only a marble texture was observed for $pPhM_{80}$. The DSC curves of the $pPhM_{80}$ homopolymer sample showed one endothermic peak at 125°C (Fig. 3); the peak can be assigned to a nematic (N) - isotropic (I) phase transition, as it was shown in our previous works.[67] In addition, the glass transition temperature of the homopolymer was observed at around 25°C.

Summarizing on the phase behavior of the two triblock copolymers, i.e. $pA_4$-*b*-$pPhM_{80}$-*b*-$pA_4$ and $pAzo_4$-*b*-$pPhM_{80}$-*b*-$pAzo_4$, it can be noted that both of them have mesophase transitions from N to I phase between 119 and 122 °C (Table 2). The presence of nematic mesophase was confirmed by POM (Fig. S10c†) and X-ray data (not shown here). In this case, X-ray scattering in the wide-angle region displays only a diffuse maximum positioned at 4.35 Å. Importantly, all block copolymers are characterized by a single glass transition temperature independent of their composition.

As it is seen from Table 2, the N-I phase transition temperatures of the block copolymers (with the exception of $pAzo_{10}$-*b*-$pPhM_{80}$-*b*-$pAzo_{10}$) are slightly lower as compared to the $pPhM_{80}$ homopolymer, forming a central subblock in the block copolymer. This means that the low content of pA and pAzo subblocks has no significant influence on the phase behavior of LC triblock copolymers, which is mainly determined by the $pPhM_{80}$ subblock. Therefore the pA and pAzo subblocks play simply a role of defects destabilizing the N phase. On the contrary, the other two block copolymers, i.e. $pA_{10}$-*b*-$pPhM_{80}$-*b*-$pA_{10}$ and $pAzo_{10}$-*b*-$pPhM_{80}$-*b*-$pAzo_{10}$, with a longer subblock of pA and pAzo show a different behavior. In POM (Fig. S10d†), the $pA_{10}$-*b*-$pPhM_{80}$-*b*-$pA_{10}$ copolymer exhibits nematic mesophase typical of pPhM block, it displays only one diffuse peak in WAXS. The DSC curves of the block copolymers are shown in Figure 5.

Two $T_g$ values were determined for the block copolymer $pA_{10}$-*b*-$pPhM_{80}$-*b*-$pA_{10}$ (Table 2) which implies a phase separation between the subblocks. The first glass transition temperature occurs at around -1°C, whereas the second one is pertinent to $T_g$ of the $pPhM_{80}$ homopolymer. The result shows that introduction

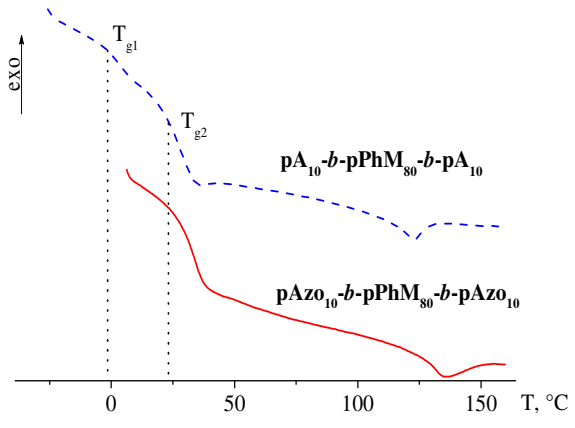


Fig. 5 DSC curves of the block copolymers obtained from the second heating scans.

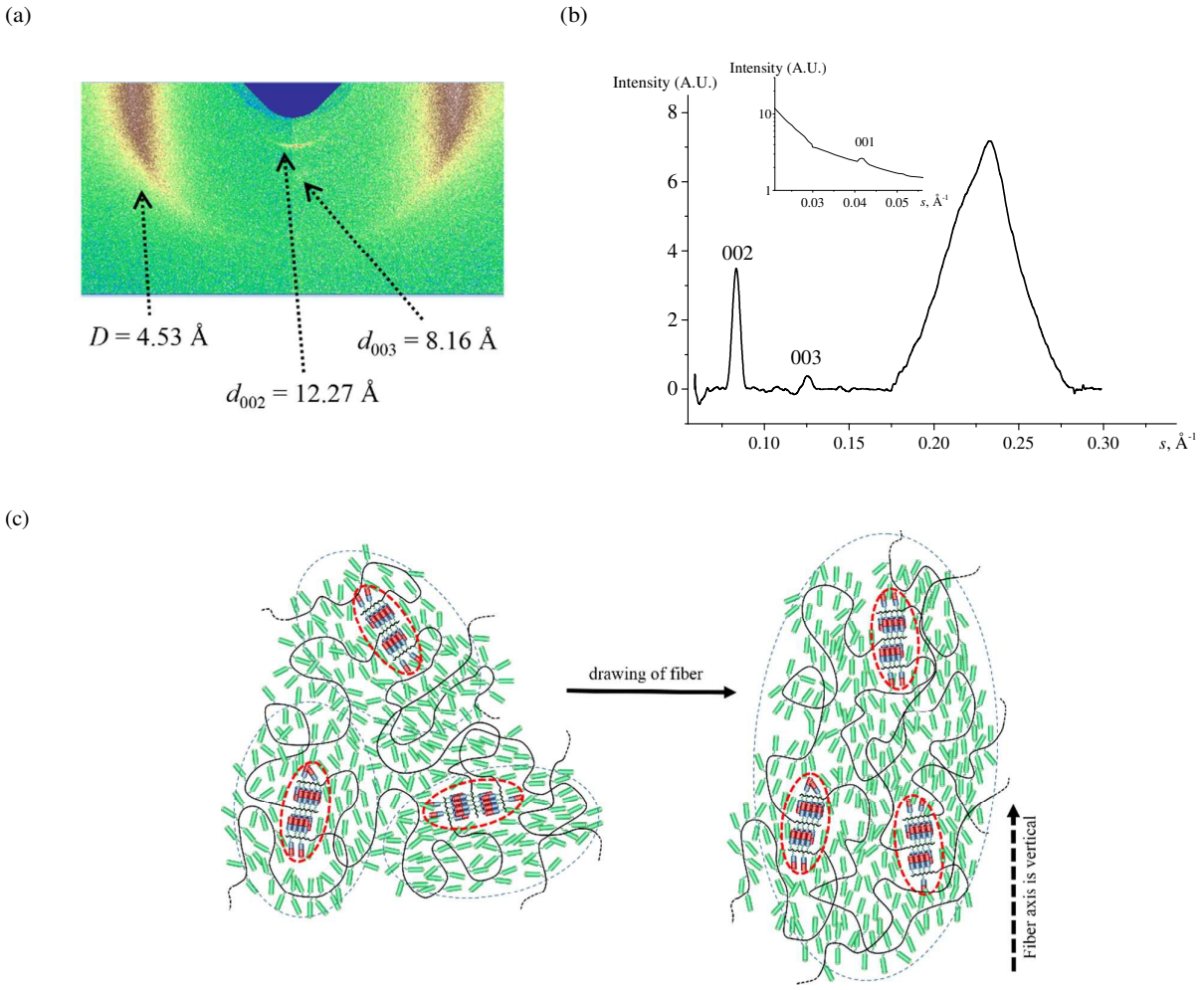


Fig. 6 (a) 2D WAXS pattern and (b) 1D WAXS and SAXS (in inset) diffractograms corresponding to $pAzo_{10}$-*b*-$pPhM_{80}$-*b*-$pAzo_{10}$. (Fiber axis is vertical. The measurement is carried out at room temperature.). (c) Schematic representation of different mesogenic group orientation during uniaxial alignment of block copolymer $pAzo_{10}$-*b*-$pPhM_{80}$-*b*-$pAzo_{10}$. The dashed line represents hypothetical domain boundaries.

of the second subblock $pPhM_{80}$ in the macromolecule can dramatically increase the glass transition temperature of the pA subblock.

The $pAzo_{10}$-*b*-$pPhM_{80}$-*b*-$pAzo_{10}$ block copolymer also shows a nematic mesophase, according to POM (Fig. S10e†) and $T_g$ around 33 °C, according to DSC measurements. The isotropization temperature of the block copolymer is higher after the formation of the Azo chromophores. Interestingly, this triblock copolymer exhibits an X-ray pattern similar to that of $pAzo_{20}$. The pattern displays three sharp scattering peaks at low angles (cf. Fig. 6), which correspond to the smectic phase and a diffuse wide-angle peak. The latter can belong to both the smectic and nematic phases, as the corresponding d-spacings are very close. It is noteworthy that we were not able to observe a microphase segregation mentioned above because the instrumental limit for the experimental setup used was around 70 Å. Importantly, although the random copolymer $pAzo_7$-*ran*-$pPhM_{30}$ has an identical percentage of the Azo groups as the block copolymer, it forms only a nematic mesophase (i.e., the small-angle reflections are absent from the SAXS profiles Fig. S10f, S11†). The comparison of the WAXS patterns corresponding to the fiber samples of the $pAzo_{20}$ homopolymer and $pAzo_{10}$-*b*-$pPhM_{80}$-*b*-$pAzo_{10}$ block copolymer shows a different orientation of the side-chain layers with respect to the fiber axis (Fig. 4 and 6). In the latter case, the layers are oriented perpendicular to the long axis of the fiber unlike homopolymer $pAzo_{20}$ (cf. the text above). To explain this, one can recall that uniaxial orientation of polymers from the nematic mesophase is accompanied by the arrangement of the mesogenic side-groups parallel to the fiber axis, whereas orientation of smectic SmA polymers results in disposition of smectic layers parallel to the direction of the mechanical field.[69] In block copolymer $pAzo_{10}$-*b*-$pPhM_{80}$-*b*-$pAzo_{10}$ the length of the block $pPhM_{80}$ forming the nematic mesophase is eight times larger than the length of the block $pAzo_{10}$ exhibiting order of the Azo groups in the smectic layers. It can be assumed that the

PhM groups make the main contribution to the orientation process, aligning along the drawing axis. As a result, the smectic layers formed by Azo groups become oriented perpendicular to the fiber axis. Schematically, the described process is represented on Fig. 6c. The results on orientation indirectly indicate that a microphase separation is present in the $pAzo_{10}$-*b*-$pPhM_{80}$-*b*-$pAzo_{10}$ block copolymer.

Moreover, the microphase-separated morphology of the block copolymer is revealed by AFM through the height images of free surfaces (Fig. 7) where the microphase-separated domain structure can be identified in the annealed films.

It is well-known that BCPs self-assemble into a range of different nanostructures, whose size can be controlled by the chain length, chemical functionality, volume fraction and the order of succession of each block.[70, 71] In the $pAzo_{10}$-*b*-$pPhM_{80}$-*b*-$pAzo_{10}$ block copolymer the pAzo subblocks form separated phases: it was counted from AFM images (Fig. 7) that a share of the space occupied by domains (21%) approximately corresponds to the contents of the Azo-groups in triblock copolymer (20%). The minority subphase formed by the pAzo blocks appears as the dark dots on the phase image. The size of observed microdomains fluctuates within 10-15 nanometers. Hence, it is possible to conclude that the domains (cylindrical or spherical form) are formed by pAzo segments, and the continuous matrix consists of $pPhM_{80}$ subblocks. The Azo groups are ordered in smectic layers inside domains, whereas the surrounding matrix represents a nematic phase formed by the $pPhM_{80}$ subblocks.

### Photoinduced processes in azobenzene-containing polymers

Photooptical and photoorientation phenomena in the photochromic polymers were studied in the dilute solutions and in the thin amorphous films obtained by spin-coating. This method allows thin homogeneous amorphous polymer films to be obtained if the glass transition temperature of polymers is higher of ambient temperature.

As have been discussed above, all synthesized azobenzene-containing polymers are characterized by the different LC phase

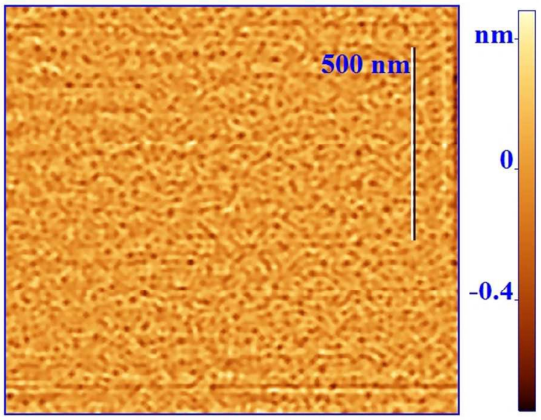


Fig. 7 AFM tapping mode height image for annealed sample of $pAzo_{10}$-*b*-$pPhM_{80}$-*b*-$pAzo_{10}$.

behavior. Taking into account this fact, the investigation of the amorphous films (in which all polymers under discussion are remaining in the same "forced" isotropic phase state) will allow us to obtain the information concerning the influence of chromophores distribution along macromolecular chain on photoinduced processes occurring in these polymers under the light action.

The plan of this section may be presented as follows. First, we will consider the optical properties and the results of studying of the photochemical transformations in solution and amorphous (isotropic) film of azobenzene-containing polymers. Then we will discuss the features of the photoorientation processes occurring in the amorphous films of homopolymer, block and random copolymers under the action of linearly polarized visible light.

**Spectral absorption data and E-Z photoisomerization processes in solutions and thin spin-coated films of photosensitive polymers.** Figure 8 shows the typical UV-vis absorbance spectra of the homopolymer $pAzo_{20}$ and block copolymer $pAzo_{10}$-*b*-$pPhM_{80}$-*b*-$pAzo_{10}$ in THF solution. Before irradiation (t = 0) the spectra showed a band centered at 442 nm corresponding to the thermodynamically stable E-isomer of the azobenzene chromophore and attributed to the π—π* and n—π* electronic transitions (the n—π* transition band is not seen in the spectrum because of overlapping with π—π* band; it clearly see from Fig. 8). This is typical for the push-pull type Azo chromophores.[72] The strong peak at around 260 nm was observed in copolymers. This peak is attributed to the superposition of azobenzene aromatic core Φ–Φ* electronic transition, π–π* and n–π* electronic transitions of phenylbenzoate chromophores. Let us mention that maximum of the absorption spectra in the interval of π—π* transition remains unchanged for all polymer solutions.

On the contrary, the spectra of thin amorphous films of homopolymer $pAzo_{20}$ and two block copolymers (Fig. 9a) are characterized by a hypsochromic shift of the π—π* absorption

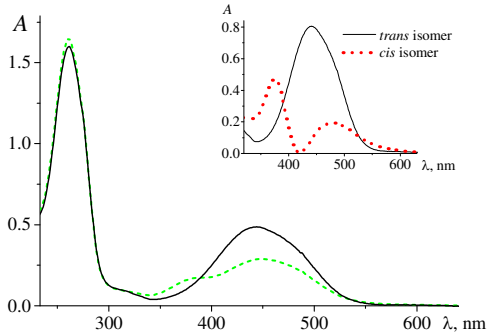


Fig. 8 UV-vis absorption spectra of block copolymer $pAzo_{10}$-*b*-$pPhM_{80}$-*b*-$pAzo_{10}$ in THF solution before (solid line) and after illumination (for 3 min) in the photostationary state(dashed line). Irradiation condition: room temperature, c =1.8 × $10^{-5}$ M, λ = 436 nm, 1.5 mW/$cm^2$. Inset shows experimental absorbance spectrum of E-isomer of the homopolymer $pAzo_{20}$ in THF solution and calculated spectral curve for its Z-isomer. The spectrum of *Z* isomer was calculated from the two spectra in the photostationary state obtained for different $\lambda_{ex}$ (404 and 436 nm) according to E. Fischer's method.[69]

(a) (b)

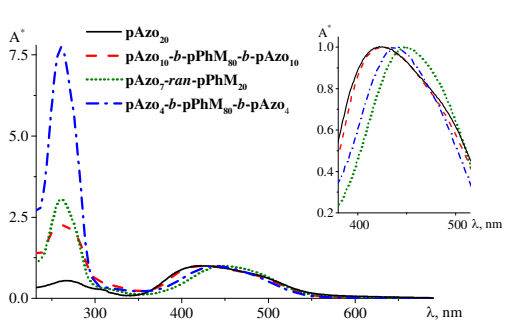


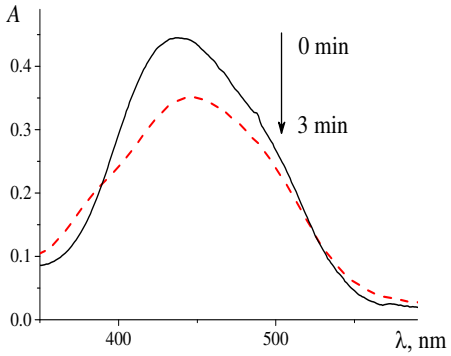


Fig. 9 (a) Absorbance spectra of as-casted amorphous homopolymer and copolymers films at room temperature normalized at maximum of π-π* electronic transition; inset shows absorbance spectra of π—π* electronic transitions of Azo chromophores in detail (A* = A / $A_{max}$, where $A_{max}$ is absorbance at maximum of π—π* electronic transition of azo chromophores); (b) changes of absorbance spectra of $pAzo_{10}$-*b*-$pPhM_{80}$-*b*-$pAzo_{10}$ copolymer film after irradiation with nonpolarized light (λ = 436 nm, 1.5 mW/$cm^2$, 22°C). Photostationary state of E-Z photoisomerization is achieved during 3 min.

maximum centered between 425 - 438 nm depending on Azo group contents in comparison with their dilute solutions ($\lambda_{max}$ = 442 nm).

Blue shift $\lambda_{max}$ indicates that in the freshly prepared films based on these polymers the formation of H-aggregates consisting of antiparallel packing of the azobenzene chromophores[72] is stronger pronounced. Let us emphasize that equal degree of chromophores aggregation is observed in polymers $pAzo_{10}$-*b*-$pPhM_{80}$-*b*-$pAzo_{10}$ and $pAzo_{20}$ (their spectra coincide, Fig. 9a). The shift $\lambda_{max}$ is less pronounced for $pAzo_4$-*b*-$pPhM_{80}$-*b*-$pAzo_4$, that indicates the smaller degree of aggregation in this copolymer (the π—π* absorption maximum centered at 438 nm).

At the same time, the dilution of azobenzene chromophores by phenylbenzoate groups in random copolymer suppresses the aggregation process. The spectrum of thin film of the random copolymer $pAzo_7$-*ran*-$pPhM_{30}$ in which Azo moieties are uniformly distributed in pPhM matrix practically coincides with its solution spectrum (the π—π* absorption maximum is centred at 444 nm). The position of this maximum corresponds apparently to nonassociated Azo-chromofores, in spite of the fact that random copolymer contains the same percentage of Azo groups similar to block copolymer $pAzo_{10}$-*b*-$pPhM_{80}$-*b*-$pAzo_{10}$.

Irradiation of polymer solutions and films with the nonpolarized light (λ = 436 nm, *I* =1.5 mW/$cm^2$) induces changes in absorption spectra of polymers which are typical for E-Z isomerization (Fig.8, 9b). It is clearly seen that an absorbance corresponding to the E isomer under irradiation decreases and a photostationary state is achieved within 3 min. A slight increase of absorbance in the range of 382 nm also takes place. This absorbance increasing is attributed to the n—π* electronic transition of the Z-isomer azobenzene chromophore whose content is increasing during the irradiation. Similar spectral features under above mention conditions (λ = 436 nm, *I* =1.5 mW/$cm^2$) were also observed for all synthesized polymers with Azo-chromophores.

We have calculated according to E. Fischer's method[62], that polymer solutions in the photostationary state contain about 50%

Table 3 E-Z isomer ratios in the photostationary state of azobenzene-containing polymers in solutions and as-casted amorphous films after irradiation (λ = 436 nm, *I* =1.5 mW/cm$^2$)

| | Z : E, %* | |
|---|---|---|
| Polymers | Solution | Film |
| $pAzo_{20}$ | 51:49 | 13:87 |
| $pAzo_{10}$-*b*-$pPhM_{80}$-*b*-$pAzo_{10}$ | 48:52 | 12:88 |
| $pAzo_4$-*b*-pPhM-*b*-$pAzo_4$ | 50:50 | 35:65 |
| $pAzo_7$-*ran*-$pPhM_{30}$ | 52:48 | 34:66 |

Z-isomer independently of molecular architecture of macromolecule. On the contrary, the considerably smaller concentration of Z-isomer is achieved in amorphous films of polymer in the photostationary state (Table 3). The latter can be explained by effects of the existence of the local free volume distribution in the polymer matrix and of the chain segmental mobility on the E-Z isomerization process.[73,74] Equally low Z-isomer content in $pAzo_{20}$ and $pAzo_{10}$-*b*-$pPhM_{80}$-*b*-$pAzo_{10}$ films is probably due to a great part H-aggregates preventing the accumulation of Z-isomer in the photostationary state.

Meanwhile content of Z-isomer is three times higher (Table 3) when the degree of aggregation is negligible ($pAzo_4$-*b*-pPhM-*b*-$pAzo_4$) or H-aggregates absent ($pAzo_7$-*ran*-$pPhM_{30}$).

Therefore, distribution of chromophores along macromolecular chain and their volume fraction have essential influence on the aggregation phenomena and E-Z isomer ratios at the photostationary state in amorphous film of azobenzene-containing polymers.

**Photoinduced optical anisotropy in spin-coated amorphous polymer films.** It is well known that majority of azobenzene-containing polymers undergo photoinduced orientational processes under illumination by polarized light. In our work light induced optical anisotropy in polymer films has been studied by the investigation of the photogenerated dichroism using linearly polarized light (546 nm, 2 mW/cm$^2$). Preliminary investigations

(a)

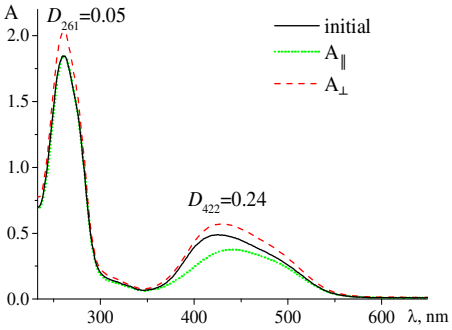


(b)

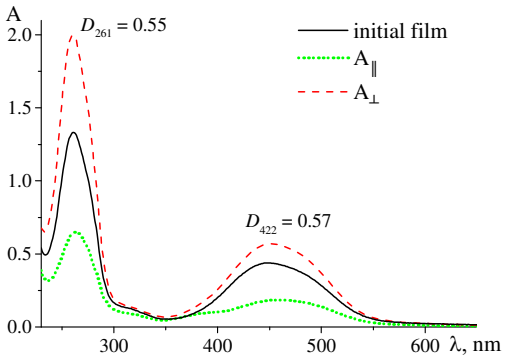


(c)

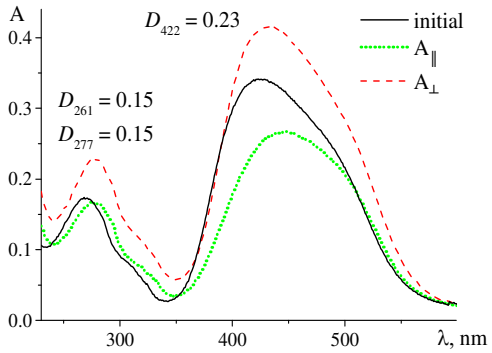


Fig. 10 Polarized absorbance spectra of the as-casted films $pAzo_{10}$-*b*-$pPhM_{80}$-*b*-$pAzo_{10}$ (a), $pAzo_7$-*ran*-$pPhM_{30}$ (b) and $pAzo_{20}$ (c) before (solid line) and after polarized light action (dash and dotted line). Irradiation conditions: 546 nm, 2 mW/cm$^2$, 22 °C. Irradiation time is equal to 1 hour for $pAzo_{10}$-*b*-$pPhM_{80}$-*b*-$pAzo_{10}$ and $pAzo_{20}$ and 5 hours for $pAzo_7$-*ran*-$pPhM_{30}$.

of the photooptical properties of amorphous polymer films of the synthesized azobenzene-containing polymers revealed, that the light exposure results in a preferred orientation of the azobenzene groups located perpendicular to the electric field vector of the linearly polarized light. As can be seen from Figure 10, polarized light absorbance for all copolymers is noticeably higher for the polarization direction perpendicular to the polarization plane of the excitation light.

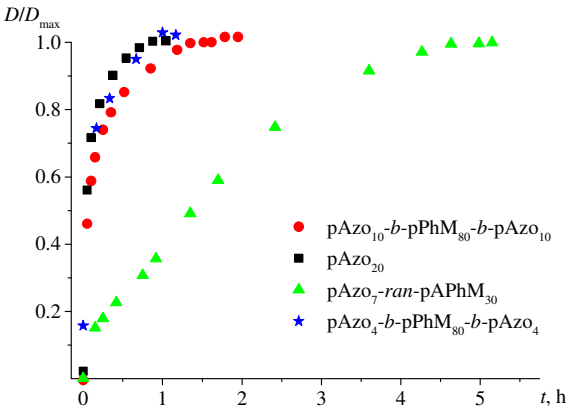


Fig. 11 Kinetics of the azobenzene chromophore dichroism (*D*) growth normalized to its maximum value ($D_{max}$) under irradiation of polymer films with polarized light (546 nm, 2 mW/cm$^2$, 22 °C).

It is noteworthy, that values of maximal achievable dichroism of the azobenzene chromophore are the same (Fig. 10a, c and S12a†) for the homopolymer $pAzo_{20}$ and block copolymer $pAzo_{10}$-*b*-$pPhM_{80}$-*b*-$pAzo_{10}$ in their amorphous films ($D$ = 0.24), while for $pAzo_4$-*b*-$pPhM_{80}$-*b*-$pAzo_4$ the dichroism value is much smaller ($D$ = 0.08, Fig. S12b†) according small concentration of the Azo groups. At the same time, among all discussed copolymers the $pAzo_7$-*ran*-$pPhM_{30}$ which contains the same percentage of Azo-groups similar to block copolymer $pAzo_{10}$-*b*-$pPhM_{80}$-*b*-$pAzo_{10}$ is characterized by the maximum value of the induced dichroism ($D$ = 0.57, Fig. 10b) among all discussed copolymers. This dichroism value is in a good agreement with

the dichroism of the well-studied azobenzene containing side chain polymers.[24] Probably, an H-aggregation of photochromic groups in homopolymer and block copolymers (Fig. 9a) studied by us partially hampers the photoorientation process decreasing the achievable values of dichroism.

Kinetics curves of linear dichroism growth normalized to its maximum value are presented in Fig. 11. They clearly demonstrated the noticeable difference in the kinetics of dichroism growth for block and random copolymers. The obtained data revealed that initial rates of the azobenzene chromophore dichroism growth are almost the same for homopolymer and all block copolymers: the dichroism value increases as a function of time and achieves maximum during about 60-80 min. Copolymer $pAzo_7$-*ran*-$PhM_{30}$ shows a completely different behavior: in the amorphous films the dichroism growth has slower evolution, in such a way that 5 hours are needed to achieve a maximum value.

Such significant di□erence could be explained by the variation in photoorientation process mechanism. Let us discuss these data in detail. As can be seen from Fig. 9 a, the E-azobenzene moieties have very small absorption in the vicinity at 260 nm, where absorption of phenyl benzoate mesogenic groups is also observed. This absorption peak becomes more pronounced with decreasing the amount of the Azo- groups with respect to $pPhM_{80}$ subblocks in copolymers (the contribution of Azo groups to the absorption peak is about 15%). Taking into account the slight absorption of Azo-groups at 260 nm, the dichroism values of phenyl benzoate mesogenic groups of copolymers have been calculated; neglecting of the Azo groups absorption (Fig. 10).

The dichroism values at 260 nm and 422 nm are practically identical for homopolymer $pAzo_{20}$ and block copolymer $pAzo_{10}$-*b*-$pPhM_{80}$-*b*-$pAzo_{10}$ (Fig. 10a and 10c). Small photoindused dichroism in the film of $pAzo_{20}$ at 260 nm is associated with orientation of Azo- groups. This result shows, that practically only Azo groups are included in the process of photoinduced orientation in spin-coated amorphous films of block copolymer $pAzo_{10}$-*b*-$pPhM_{80}$-*b*-$pAzo_{10}$. In other words the subblocks $pPhM_{80}$ do not participate in this process and do not prevent to orientation of the pAzo subblocks.

On the contrary, in the case of random copolymer $pAzo_7$-*ran*-$pPhM_{30}$, the dichroism values at 260 nm and 422 nm are equal and significantly large than for block copolymer $pAzo_{10}$-*b*-$pPhM_{80}$-*b*-$pAzo_{10}$. This means, that the orientational cooperative effect of the both azobenzene chromophore and phenyl benzoate mesogenic groups is observed. The same situation was usually observed for a majority of azobenzene copolymers described in the literature.[24]

## Conclusions

A novel synthetic route allowing to obtain symmetrical photosensitive fully liquid crystalline side chain triblock copolymers and random copolymer with nematogenic phenyl benzoate and photosensitive azobenzene containing mesogenic groups that combines RAFT polymerization and subsequent chemical modification has been developed. The results of the polymerization of acrylic monomer A with methylaniline groups proved that S,S'-bis(methyl-2-isobutyrate) trithiocarbonate is an effective RAFT agent. The $^1$H NMR and chain extension results confirmed RAFT process of such polymerization. The central block of synthesized photochromic block copolymers contains 80 phenyl benzoate mesogenic groups (PhM), while the length of "peripheral" blocks includes 4 or 10 azobenzene (Azo) units. Random copolymer with the same mesogenic units, "basic" homopolymers and block copolymers, containing methylaniline (A) groups using in azocoupling reaction have been also synthesized as reference samples. The results demonstrated that microphase separation structure is observed in block copolymers when the length of subblock with Azo and A groups reaches ten monomeric units. It was shown, that distribution of chromophores along macromolecular chain and their volume fraction have essential influence on the aggregation phenomena, isomerization ratios at the photostationary state and mechanism of their photoorientation in amorphous film of Azo-containing polymers. The dichroism growth kinetics in amorphous copolymers films is studied and an influence of polymers molecular architecture on the photoinduced dichroism is revealed. This study shows that practically only Azo groups are included in the process of photoinduced orientation in spin-coated amorphous films of block copolymer, whereas the

orientational cooperative effect of both azobenzene chromophore and phenyl benzoate mesogenic groups is observed only in the case of random copolymer.

## Acknowledgements

This research was financially supported by the Russian Science Foundation (Grant №14-13-00379) – synthesis of polymers, thermal behavior, photochemical and photooptical studies and by Russian Ministry of Science and Education (project №11.G34.31.0055) –X-ray analysis. The authors are grateful to Olga Sinitsyna for helpful discussions.

## References

1 Ikeda T, Zhao Y. Smart Light-Responsive Materials: Azobenzene Containing Polymers and Liquid Crystals, John Wiley & Sons Inc, Hoboken, New Jersey; 2009.
2 H. Ringsdorf, H.W. Schmidt, H. Eilingsfeld, K.H. Etzbach. *Makromol. Chem.*, 1987, **188**, 1355–1366.
3 S. Hvilsted, F. Andruzzi, C. Kulinna, H. W. Siesler and P. S. Ramanujam, *Macromolecules*, 1995, **28**, 2172–2183.
4 B. Tylkowski, S. Peris, M. Giamberini, R. Garcia-Valls, J. A. Reina and J. C. Ronda, *Langmuir*, 2010, **26**, 14821−14829.
5 X. Pei, A. Fernandes, B. Mathy, X. Laloyaux, B. Nysten, O. Riant and A. M. Jonas, *Langmuir*, 2011, **27**, 9403−9412.
6 T. Ikeda, S. Horiuchi, D. B. Karanjit, S. Kurihara and S. Tazuke, *Macromolecules*, 1990, **23**, 42−48.
7 B. Zupancic, S. Diez-Berart, D. Finotello, O. D. Lavrentovich and B. Zalar, *Phys. Rev. Lett.*, 2012, **108**, 257801.
8 P. V. Dolganov, E. I. Demikhov, V. K. Dolganov, B. M. Bolotin and K. Krohn, *Eur. Phys. J. E*, 2003, **12**, 593−597.
9 S. K. Prasad, *Mol. Cryst. Liq. Cryst*, 2009, **509**, 317−327.
10 H. Finkelmann, E. Nishikawa, G. G. Pereira and M. Warner, *Phys. Rev. Lett.*, 2001, **87(1)**, 015501.
11 Y. L. Yu, M. Nakano and T. Ikeda, *Nature*, 2003, **425(6954)**, 145.
12 M. H. Li, P. Keller, B. Li, X. G. Wang and M. Brunet, *Adv. Mater*, 2003, **15(7-8)**, 569−72.
13 A. Shimamura, A. Priimagi, J. Mamiya, T. Ikeda, Y. Yu, C. J. Barrett and A. Shishido, *Appl. Mater. Interfaces*, 2011, **3**, 4190−4196.
14 K. M. Lee, D. H. Wang, H. Koerner, R. A. Vaia, L. S. Tan and T. White, *J. Angew. Chem. Int. Ed.,* 2012, **51**, 4117–4121.
15 K. M. Lee and T. J. White, *Macromolecules*, 2012, **45**, 7163−7170.
16 K. M. Lee, N. V. Tabiryan, T. J. Bunning and T. J. White, *J. Mater. Chem.,* 2012, **22**, 691−698.
17 A. Ryabchun, A. Bobrovsky, J. Stumpe and V. Shibaev, *Macromol. Rapid. Commun*., 2012, **33**, 991−997.
18 D. Y. Kim, S. K. Tripathy and L. Li, J. Kumar, *Appl. Phys. Lett.*, 1995, **66(10)**, 1166−8.
19 P. Rochon, E. Batalla and A. Natansohn, *Appl. Phys. Lett.*, 1995, **66(2)**, 136−8.
20 D. Kessler, F. D. Jochum, J. Choi, K. Char and P. Theato, *Appl. Mater. Interfaces*, 2011, **3**, 124−128.
21 F. Weigert, *Werhandlungen der Deutschen Physikalischen Gesellschaft*, 1919, **21**, 479.
22 M. Eich and J. H. Wendorff, *Makromol. Chem. Rapid. Commun.*, 1987, **8**, 467−471.
23 Shibaev V. Polymers as Electrooptical and Photooptical Active Media, Springer-Verlag Berlin-Heidelberg-New-York, 1996.
24 V. Shibaev, A. Bobrovsky and N. Boiko, *Prog. Polym. Sci.*, 2003, **28(5)**, 729-836.
25 A. Natansohn and P. Rochon, *Chem. Rev.*, 2002, **102(11)**, 4139−75.
26 J. A. Delaire and K. Nakatani, *Chem. Rev.*, 2000, **100(5)**, 1817−45.
27 K. Ichimura, *Chem. Rev.*, 2000, **100**, 1847−1874.
28 M. J. Kim, S. J. Yoo and D. Y. Kim, *Adv. Funct. Mater.*, 2006, **16**, 2089−2094.
29 J. Kumar, L. Li, X. L. Jiang, D. Kim, T. S. Lee and S. Tripathy, *Appl. Phys. Lett*., 1998, **72**, 2096−2098.
30 R. H. Berg, S. Hvilsted and P. S. Ramanujam, *Nature*, 1996, **383(6600)**, 505−508.
31 S. J. Zilker, M. R. Huber, R. Bieringer and D. Haarer, *Appl. Phys. B*, 1999, **68**, 893−897.
32 F. Ercole, T. P. Davis and R. A. Evans, *Polym. Chem.,* 2010, **1**, 37–54.
33 S. Kadota, K. Aoki, S. Nagano and T. Seki, *J. Am. Chem. Soc*., 2005, **127**, 8266−8267.
34 H. Yu, K. Okano, A. Shishido, T. Ikeda, K. Kamata, M. Komura and T. Iyoda, *Adv. Mater*., 2005, **17**, 2184−2188.
35 K. Aoki, T. Iwata, S. Nagano and T. Seki, Macromol. *Chem. Phys.*, 2010, **211**, 2484–2489.
36 H. F. Yu, A. Shishido, T. Iyoda and T. Ikeda, *Macromol. Rapid. Commun.,* 2007, **28**, 927–931.
37 C. Berges, I. r. Javakhishvili, S. Hvilsted, C. Sánchez and R. Alcalá, *Macromol. Chem. Phys.*, 2012, **213,** 2299−2310.
38 Yu. Zhu, Yu. Zhou, Zh. Chen, R. Lin and Xi. Wang, *Polymer*, 2012, **53**, 3566−3576.
39 C. F. Huang, W. Chen, T. P. Russell, A. C. Balazs, F. C. Chang and K. Matyjaszewski, *Macromol. Chem. Phys*., 2009, **210**, 1484−1492.
40 Q. Yan, D. Han, Yu. Zhao, *Polym. Chem.*, 2013, **19**, 5026−5037.
41 Ja. Heo, Yu. J. Kim, M. Seo, S. Shin and S. Y. Kim, *Chem. Commun*., 2012, **48**, 3351–3353.
42 A. Bobrovsky, N. Boiko, V. Shibaev, *Polymer*, 2015, **56**, 263−270.
43 V. Shibaev, N. Boiko in Silicon-containing dendritic polymers. P.R Dvornic, M.J Owen (editors), 237 Advances in Silicon Science 2, Springer Science, Business Media B.V; 2009.
44 S. Hernandez-Ainsa, R. Alcala, J. Barbera, M. Marcos, C. Sanchez, J. L. Serrano, *Macromolecules*, 2010, **43**, 2660–2663.
45 E. Blasco, M. Piñol and L. Oriol, *Macromol. Rapid. Commun*., 2014, **35**, 1090−1115.
46 R. Deloncle and A. M. Caminade, *J. Photochem. Photobiol. C. Photochem. Rev*., 2010, **11**, 25–45.
47 Y. Morikawa, T. Kondo, S. Nagano and T. Seki, *Chem. Mater*., 2007, **19**, 1540–1542.
48 S. Nagano, Y. Koizuka, T. Murase, M. Sano, Y. Shinohara, Y. Amemiya and T. Seki, *Angew. Chem. Int. Ed*., 2012, **51**, 5884.
49 Yu. Zhu and X. Wang, *Dyes and Pigments*, 2013, **97**, 222−229.
50 Y. Zhao, X. Tong and Y. Zhao, *Macromol. Rapid. Commun*., 2010, **31**, 986–990.
51 Yi Zhao, Bo Qi, X. Tong and Y. Zhao, *Macromolecules*, 2008, **41(11)**, 3823−3831.
52 A. Natansohn, P. Rochon, X. Meng, C. Barrett, T. Buffeteau, S. Bonenfantand and M. Pe´zolet, *Macromolecules*, 1998, **31**, 1155−1161.
53 A. Natansohn and P. Rochon, *Chem. Rev*., 2002, **102(11)**, 4139−75.
54 T. Todorov, L. Nikolova and N. Tomova, *Appl. Opt.*, 1984, **23(23)**, 4309-4312.

55 X. G. Wang, J. I. Chen, S. Marturunkakul, L. Li, J. Kumar and S. K. Tripathy, *Chem. Mater*., 1997, **9(1)**, 45–50.
56 X. G. Wang, J. Kumar, S. K. Tripathy, L. Li, J. I. Chen and S. Marturunkakul, *Macromolecules*, 1997, **30(2)**, 219–225.
57 I. A. Budagovsky, A. S. Zolot'ko, T. E. Koval'skaya, M. P. Smayev, S. A. Shvetsov, N. I. Boiko, M. A. Bugakov and M. I. *Barnik, Bull. Lebedev. Phys. Institute*, 2014, **41(5)**, 135–139.
58 M. A. Bugakov, N. I. Boiko, E. V. Chernikova and V. P. Shibaev, *Polym. Sci. B*, 2013, **55(5–6)**, 294–303.
59 E. V. Chernikova, Z. A. Poteryaeva, S. S. Belyaev, I. E. Nifant'ev, A. V. Shlyakhtin, Y. u. V. Kostina, A. S. Cherevan', M. N. Efimov, G. N. Bondarenko and E. V. Sivtsov, *Polym. Sci. B*, 2011, **53**, 391–395.
60 N. Boiko, V. Shibaev and M. Kozlovsky, *J. Polym. Sci. B. Polym. Phys*., 2005, **43**, 2352–2360.
61 D. Wang, G. Ye and X. Wang, *Macromol. Rapid. Commun*., 2007, **28**, 2237–2243.
62 E. Fisher, *J. Phys. Chem*., 1967, **71(11**), 3704–3706.
63 M. G. Ivanov, N. I. Boiko, E. V. Chernikova, R. Richardson, X. M. Zhu and V. P. Shibaev, *Polym. Sci. A*, 2011, **53**, 633–644.
64 E.V. Chernikova, D.V. Vishnevetskii, E.S. Garina, A.V. Plutalova, E.A. Litmanovich, B.A. Korolev, A.V. Shlyakhtin, Yu.V.Kostina and G.N. Bondarenko, *Polym. Sci. B*, 2012, **54**, 127–141.
65 L. Manfred, H. Hallensleben and B. Weichart, *Polym. Bull.*, 1989, **22**, 557-563.
66 G. Moad, E. Rizzardo and S. H. Thang, *Polymer*, 2008, **49**, 1079–1131.
67 G. Odian Principles of Polymerization, John Wiley & Sons Inc, New York, 2004.
68 G. Moad, E. Rizzardo, and S. H. Thang, *Aust. J. Chem.*, 2006, **59**, 669-692.
69 Y. S. Freidzon, R. V. Talroze, N. I. Boiko, S. G. Kostromin, V. P. Shibaev and N. A. Plate, *Liq. Cryst*., 1988, **3(1)**, 127–132.
70 M. R. Bockstaller, R. A. Mickiewicz and E. L. Thomas, *Ad. Mater*., 2005, **17**, 1331–1349.
71 G. H. Fredrickson, *Phys. Today*, 1999, **52**, 32–40.
72 F. L. Labarthet, S. Freiberg, C. h. Pellerin, M. Pe´zolet and A. Natansohn, P. Rochon, *Macromolecules*, 2000, **33**, 6815–6823.
73 C. D. Eisenbach, *Makromol. Chem*., 1978, **179**, 2489–2506.
74 I. Mita, K. Horie and K. Hirao, *Macromolecules*, 1989, **22**, 558–563.

Photosensitive random and triblock copolymer (TBC)

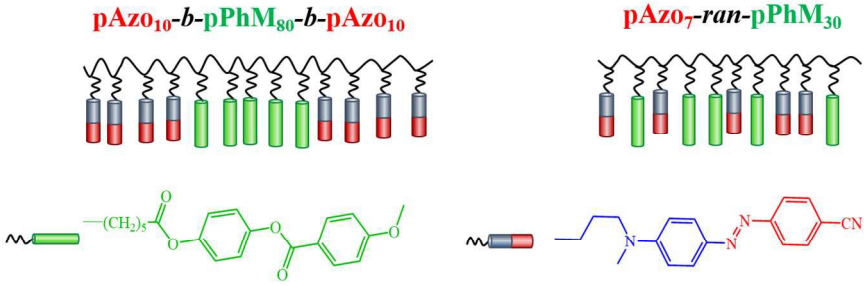


Uniaxial fiber structure of TBC

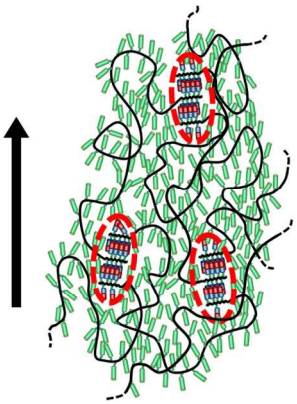

Time dependence of reduced photoinduced dichroism ($D/D_{max}$)